Fracture Mechanics of Concrete and Concrete Structures -
Recent Advances in Fracture Mechanics of Concrete - B. H. Oh, et al.(eds)

Cohesive-overlapping crack model describing the size-scale effects on the rotational capacity of RC beams in bending

M. Corrado, M. Paggi & A. Carpinteri
Politecnico di Torino, Torino, Italy

ABSTRACT: A numerical algorithm is proposed for the prediction of the mechanical behavior of the plastic hinges taking place in RC beams at the ultimate loading conditions. The main novelty of such an approach is the introduction of the *Overlapping Crack Model*, based on nonlinear fracture mechanics concepts, to describe concrete crushing, along with the well-known *Cohesive Crack Model* for concrete in tension and a stress versus crack opening displacement relationship for steel reinforcement. As a result of a systematic application of the proposed algorithm, new practical design diagrams are proposed for the improvement of the current codes of practice, which completely disregard the size-scale effects. In this context, Dimensional Analysis is also applied in order to obtain further simplifications in the description of the overall response. It is in fact demonstrated that only two nondimensional numbers, N_P and N_C, are responsible for the available ductility. A new interpretation of the experimental results on the plastic rotations in terms of N_P and N_C is also proposed.

1 INTRODUCTION

A detailed analysis of the mechanical behavior of reinforced concrete structures during the loading process evidences a series of complex phenomena characterizing the global nonlinearity, namely concrete fracturing and/or crushing and steel yielding and/or slippage. Aiming at providing an accurate description of the flexural response of reinforced concrete beams, Carpinteri et al. (2007, 2009) proposed a numerical model based on fracture mechanics concepts. In particular, the concrete fracturing is described by means of the well-known *Cohesive Crack Model*, whereas the original *Overlapping Crack Model* has been introduced for concrete crushing. According to the latter model, the concrete damage in compression is represented by means of a fictitious interpenetration. The larger is the interpenetration, the lower are the transferred forces across the damaged zone. An elasto-plastic stress versus crack opening displacement relationship describing the steel reinforcement behavior is also integrated into the numerical algorithm. By applying such a numerical model it has been possible to simulate the moment versus rotation diagrams of several experimental tests and to investigate on the rotational capacity by varying all the mechanical and geometrical parameters, in particular by addressing the issue of size-scale effects (Carpinteri et al. 2007, 2009a, b).

However, due to the presence of lots of variables and several nonlinearities, it is impossible to propose a synthetic description of the physical phenomenon. From the theoretical point of view, in fact, the problem of the rotational capacity of reinforced concrete beams has been faced by several models developed in the last decades, each of them focusing on a different aspect: steel ductility and steel-concrete interaction (Langer 1998, Bigaj & Walraven 1993), concrete strain localization in tension and compression (Bigaj & Walraven 1993, Hillerborg 1990), tension-stiffening (Cosenza et al. 1991), shear effect (Pommerening 1996). Analogously, experimental tests have been carried out in order to investigate the effect of one parameter at a time on the plastic hinges: the steel ductility (Eligehausen & Langer 1987, Calvi et al. 1993, Beeby 1997), the concrete compressive strength (Shin et al. 1989, Markeset 1993, Pecce & Fabbrocino 1999), the reinforcement in the compressive zone (Burns & Siess 1966), the confinement of concrete by means of stirrups (Burns & Siess 1966, Somes 1966), as well as the structural dimension (Mattock 1965, Corley 1966, Bigaj & Walraven 1993, Bosco & Debernardi 1993). This makes difficult the interpretation of the experimental results and reduces the prediction capability of analytical models. So far, for instance, the relative neutral axis position at the ultimate condition, x/d, has been chosen as a governing parameter for the rotational capacity. According to this choice, the results of different experimental campaigns have been merged in a ϑ_{PL} versus x/d diagram, as an attempt to obtain a practical design prescription. However, the wide scattering of the results in such a diagram, clearly evidenced in (Siviero 1974), suggests that the nondimensional parameter x/d does not completely describe the considered phenomenon.

In order to overcome such drawbacks, relevant contributions are given by Dimensional Analysis based on the Buckingham's Π-Theorem (Buckingham 1915). The application of such a procedure to structural analysis, in fact, permits to clearly connect the mechanical response to dimensionless groups of the variables involved in the phenomenon, rather than to the individual values of them. Applications of dimensional analysis to Linear Elastic Fracture Mechanics have been proposed by Carpinteri since 1981, in order to study the stability of progressive cracking in brittle materials and in reinforced concrete elements (Carpinteri 1981a, b, c, 1982), and to evaluate the minimum reinforcement necessary to avoid unstable crack propagation (Bosco & Carpinteri 1992). In the case of brittle materials, the fracturing phenomenon is governed by the following nondimensional parameter, also called stress brittleness number (Carpinteri 1981a, b, c):

$$s = \frac{K_{IC}}{\sigma_u h^{1/2}} \tag{1}$$

where K_{IC} is the material fracture toughness, σ_u is its ultimate strength and h is a characteristic linear size of the specimen. A transition from ductile to brittle failure is predicted by decreasing the brittleness number, s. In the case of lightly reinforced concrete elements, instead, a different nondimensional parameter has been introduced (Carpinteri 1982, 1984):

$$N_P = \rho \frac{\sigma_y h^{1/2}}{K_{IC}} \tag{2}$$

where ρ and σ_y are, respectively, the percentage and the yielding strength of steel reinforcement. Also in this case, a ductile-to-brittle transition occurs by decreasing the reinforcement brittleness number, N_P. Finally, the application of dimensional analysis to Nonlinear Fracture Mechanics, and in particular to the Cohesive Crack Model, permitted to introduce the energy brittleness number (Carpinteri 1985, 1991):

$$s_E = \frac{\mathcal{G}_F}{\sigma_u h} \tag{3}$$

where $\mathcal{G}_F$ is the fracture energy. Analogously to the previous numbers, a transition from ductile to softening, or even snap-back, failure is evidenced by decreasing s_E. More recently, the dimensional analysis has been applied to the *Bridged Crack Model* in order to analyse the failure mechanism transition, from flexural to shear and crushing, in reinforced and fibre-reinforced concrete beams (Carpinteri et al. 2003), and to a best-fitting procedure for the prediction of the compressive strength of concrete specimens (Phatak & Desphande 2005) and the ultimate torsional capacity of reinforced concrete beams (Phatak & Dhonde 2003).

In the present paper, Dimensional Analysis is applied, contextually to the model proposed by Carpinteri et al. (2007, 2009), for the assessment of the rotational capacity of reinforced concrete beams in bending. In particular, it will be demonstrated that only two nondimensional parameters, N_P and N_C, are responsible for the available ductility. Then, experimental confirmations of the numerical approach are also proposed.

2 NUMERICAL INVESTIGATION

In this section, the numerical algorithm proposed by Carpinteri et al. (2007, 2009) for the analysis of the behavior of reinforced concrete elements in bending is briefly described. This model permits to study a portion of a reinforced concrete beam subjected to a constant bending moment M. This element, having a span to depth ratio equal to unity, is representative of the zone of a beam where a plastic hinge formation takes place. It is assumed that fracturing and crushing are fully localized along the mid-span cross-section of the element. This assumption, fully consistent with the crushing phenomenon, also implies that only one equivalent main tensile crack is considered. The loading process is characterized by crack propagation in tension, steel yielding and/or slippage, and concrete crushing in compression.

In the proposed algorithm, the behaviour of concrete in tension is described by means of the well established Cohesive Crack Model (Hillerborg et al. 1976, Carpinteri 1985, 1989), largely used, in the past, to study the ductile-to-brittle transition in plain concrete beams in bending. According to this model, the adopted constitutive law is a stress–strain linear-elastic relationship up to the achievement of the tensile strength, σ_u, for the undamaged zone, and a stress–displacement relationship describing the material in the process zone. In particular, the cohesive stresses are considered to be linearly decreasing functions of the crack opening, w^t. The critical crack opening displacement is equal to $w^t_{cr} \approx 0.1$ mm, and the fracture energy, $\mathcal{G}_F$, is assumed to vary from 0.050 N/mm to 0.150 N/mm, depending on concrete strength and maximum aggregate diameter, according to the prescriptions given in the Model Code 90 (1993).

As far as modelling of concrete crushing failure is concerned, the Overlapping Crack Model introduced by Carpinteri et al. (2007, 2009) is adopted. According to such an approach, strongly confirmed by experimental results (van Mier 1984, Jansen & Shah 1997), and derived from the pioneering work by Hillerborg (1990), the inelastic deformation in the post-peak regime is described by a fictitious interpenetration of the material, while the remaining part of the specimen undergoes an elastic unloading. As a result, a pair of constitutive laws for concrete in compression is introduced, in close analogy with the Cohesive Crack Model: a stress-strain relationship until the compression strength is achieved (Fig. 2a), and a stress-displacement (*overlapping*) relationship describing the phenomenon of concrete crushing (Fig. 2b). The latter law describes how the stress in the damaged material decreases from its maximum value to zero as the fictitious interpenetration increases from zero to the critical value, w_{cr}^{c}. It is worth noting that the crushing energy, $\mathcal{G}_C$, which is a dissipated surface energy, defined as the area below the post-peak softening curve in Figure 2b, can be assumed as a true material property, since it is not affected by the structural size. An empirical equation for calculating the crushing energy has been recently proposed by Suzuki et al. (2006), taking into account the lateral confinement exerted by stirrups. By varying the concrete compressive strength from 20 to 90 MPa, the crushing energy ranges from 30 to 58 N/mm. The critical value for the crushing interpenetration is experimentally found to be approximately equal to w_{cr}^{c} ≈ 1 mm (see also Jansen & Shah 1997). It is worth noting that this value is a decreasing function of the compressive strength, whereas it increases by increasing the concrete confinement.

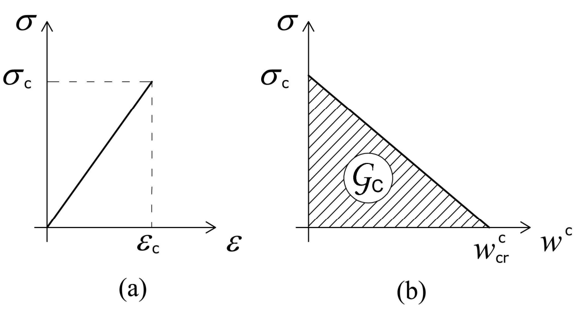

Figure 1. Overlapping Crack Model for concrete in compression: linear-elastic σ–ε law (a); post-peak softening σ–w relationship (b).

As far as the behaviour of steel reinforcement is concerned, it is impossible to adopt the classical σ–ε laws, since the kinematics of the mid-span cross-section of the reinforced concrete member is described by means of displacements, instead of strains. To this aim, constitutive relationships between the reinforcement reaction and the crack opening displacement are obtained by means of preliminary studies carried out on the interaction between the reinforcing bar and the surrounding concrete. In particular, the integration of the differential slips over the transfer length, l_{tr}, is equal to half the crack opening at the reinforcement level, whereas the integration of the bond stresses gives the reinforcement reaction. Simplified procedures of such an approach have been proposed by Ruiz et al. (1999) and Brincker et al. (1999). Typically, the obtained relationships are characterized by an ascending branch up to steel yielding, to which corresponds the critical value of the crack opening for steel, w_y. After that, the steel reaction is nearly constant.

2.1. *Numerical Algorithm*

A discrete form of the elastic equations governing the mechanical response of the two half-beams is herein introduced. The reinforced concrete member is considered as constituted by two symmetrical elements characterised by an elastic behaviour, and connected by means of *n* pairs of nodes (Figure 2a). In this approach, all the mechanical nonlinearities are localised in the mid-span cross-section, where cohesive and overlapping stresses are replaced by equivalent nodal forces, F_i, by integrating the corresponding stresses over the nodal spacing. Such nodal forces depend on the nodal opening or closing displacements according to the cohesive or overlapping softening laws previously introduced.

With reference to Figure 2a, the horizontal forces, F_i, acting at the i-th node along the mid-span cross-section, can be computed as follows:

$$\{F\} = [K_w]\{w\} + \{K_M\} M \tag{4}$$

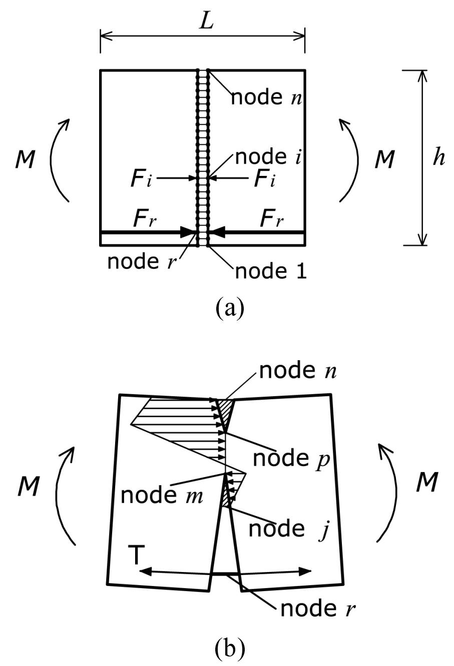

Figure 2. Finite element nodes (a); and force distribution with cohesive crack in tension and crushing in compression (b) along the mid-span cross-section.

where: $\{F\}$ is the vector of nodal forces, $[K_w]$ is the matrix of the coefficients of influence for the nodal displacements, $\{w\}$ is the vector of nodal displacements, $\{K_M\}$ is the vector of the coefficients of influence for the applied moment M.

In the generic situation shown in Figure 4b, the following equations can be considered:

$$F_i = 0\,; \text{for i} = 1, 2, \ldots, (j-1); \quad i \neq r \tag{5a}$$

$$F_i = F_u\left(1-\frac{w_i^t}{w_{cr}^t}\right); \text{ for i} = j, \ldots, (m-1); \quad i \neq r \tag{5b}$$

$$w_i = 0\,; \text{ for i} = m, \ldots, p \tag{5c}$$

$$F_i = F_c\left(1-\frac{w_i^c}{w_{cr}^c}\right); \text{ for i} = (p+1), \ldots, n \tag{5d}$$

$$F_i = f\left(w_i\right); \text{ for i} = r. \tag{5e}$$

where: j represents the real crack tip, m represents the fictitious crack tip, p is the fictitious overlapping tip and r is the node corresponding to the steel reinforcement (see Fig. 4b). The reinforcement contribution is included in the nodal force corresponding to the r-th node (see Eq. (5e)).

Equations (4) and (5) constitute a linear algebraic system of ($2n$) equations in ($2n$+1) unknowns, namely $\{F\}$, $\{w\}$ and M. The necessary additional equation derives from the strength criterion adopted for tensile crack or crushing zone propagation. At each step of the loading process, in fact, either the force in the fictitious crack tip, m, equals the ultimate tensile force, or the force in the fictitious crushing tip, p, equals the ultimate compressive force. It is important to note that the condition for crack propagation (corresponding to the achievement of the tensile strength at the fictitious crack tip, m) does not imply that the compressive strength is reached at the corresponding overlapping crack tip, p, and viceversa. Hence, the driving parameter of the process is the tip that in the considered step has reached the limit resistance. Only this tip is moved when passing to the next step. This criterion will ensure the uniqueness of the solution on the basis of physical arguments.

Finally, at each step of the algorithm, it is possible to calculate the beam rotation, ϑ, as follows:

$$\vartheta = \{D_w\}^T\{w\} + D_M M \tag{6}$$

where $\{D_w\}$ is the vector of the coefficients of influence for the nodal displacements, and D_M is the coefficient of influence for the applied moment.

It is worth noting that Eqs. (4) and (6) permit to analyse the fracturing and crushing processes of the mid-span cross-section taking into account the elastic behaviour of the reinforced concrete member. To this aim, all the coefficients are computed *a priori* using a finite element analysis. Due to the symmetry of the problem, a homogeneous concrete rectangular region, corresponding to half the tested specimen shown in Figure 2a, is discretized by means of quadrilateral plane stress elements with uniform nodal spacing. Horizontal constraints are then applied to the nodes along the vertical symmetry edge. The coefficients $K_w^{i,j}$ entering Equation (4), which relate the nodal force F_j to the nodal displacement w_i, have the physical dimensions of a stiffness and are computed by imposing a unitary horizontal displacement to each of the constrained nodes. On the other hand, by applying a unitary external bending moment, it is possible to compute the coefficients K_M^i. At the same time, each coefficient of influence for the nodal displacement on the global rotation, D_w^i, is given by the rotation of the free edge corresponding to a unitary displacement of the i-th constrained node. Finally, D_M is the rotation of the free edge corresponding to a unitary external bending moment.

3 NEW PROPOSAL FOR DESIGN CODES

In this section, the results of a detailed parametric study carried out in order to analyze the effect of each parameter to the overall response are presented, with particular regard to the plastic rotational capacity. With reference to the typical moment versus rotation curve obtained by the application of the proposed algorithm shown in Figure 3, the plastic component of the total rotation can be obtained as the difference between the ultimate rotation and the rotation corresponding to the reinforcement yielding. According to the definition proposed by Hillerborg (1990) and Pecce (1997), the ultimate rotation is the rotation beyond which the moment starts descending rapidly.

The results of the parametric analysis can be summarized in a plastic rotation versus relative neutral axis position, x/d, diagram. This is also consistent with the practical prescriptions of the Eurocode 2 (CEN TC/250 2004). The numerical results referred to different beam depths are compared in Figure 4 with the curve provided by Eurocode 2 for high ductility steel and concrete compressive strength less than or equal to 50 MPa. Beams with a depth equal to 0.2 m have a rotational capacity greater than that suggested by the code. On the other hand, by increasing the beam depth up to 0.6 or 0.8 m, the rotations provided by the code appear to be not conservative. It is worth noting that the numerical results are however in good agreement with the curve provided by the code, because the latter was calibrated on a large series of tests carried out on beams with depth of about 0.3 m.

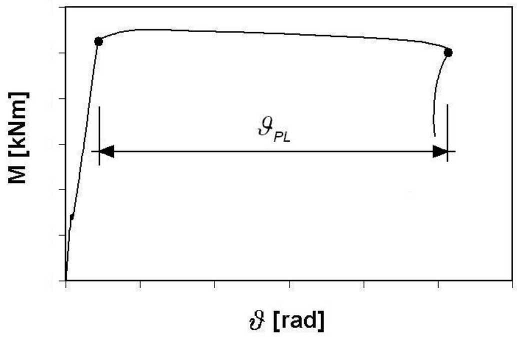

Figure 3. Definition of plastic rotation.

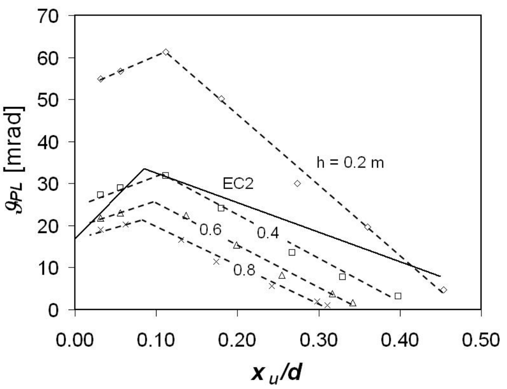

Figure 4. Numerical plastic rotation for different beam depths (dotted lines) compared with the Eurocode 2 provision (solid line).

4 APPLICATION OF DIMENSIONAL ANALYSIS TO THE FLEXURAL BEHAVIOUR OF RC BEAMS

The most relevant applications of Dimensional Analysis in Solids Mechanics have concerned the analysis of complete and incomplete physical similarity of strength and toughness in disordered materials (Carpinteri 1981a, b, c, 1982, 1984, 1991, Carpinteri et al. 2003, Phatak & Dhonde 2003, Phatak & Deshpande 2005) as well as the study of the incomplete self-similarity in fatigue crack growth (Barenblatt & Botvina 1980, Ciavarella et al. 2008).

When the flexural behavior of reinforced concrete beams is studied according to the numerical model proposed in the previous section, the functional relationship among the quantities characterizing the phenomenon is the following:

$$M = \Phi\ (\sigma_u, \mathcal{G}_F, \sigma_c, \mathcal{G}_C, E_c, \sigma_y, \rho_t, h; b/h, L/h, \vartheta), \quad (7)$$

where M is the resistant bending moment, σ_u, $\mathcal{G}_F$, σ_c, $\mathcal{G}_C$, E_c are, respectively, the tensile strength, the fracture energy, the compressive strength, the crushing energy, and the elastic modulus of concrete; σ_y and ρ_t represent the yield strength and the percentage of the tensile reinforcement, h is the characteristic size of the body, b/h and L/h define the geometry of the sample according to Figure 1, and ϑ is the local rotation of the element. Since we are interested in the rotational capacity of over-reinforced concrete beams, the set of variables can be simplified as follows:

$$M = \Phi\ (\sigma_c, \mathcal{G}_C, E_c, \sigma_y, \rho_t, h; \vartheta) \quad (8)$$

where the parameters describing the behavior of concrete in tension, σ_u and $\mathcal{G}_F$, are not explicitly considered, since they affect only the ascending branch of the moment versus rotation response and do not influence the level and the extension of the plastic plateau. On the other hand, only the beam depth, h, is considered, since the geometrical ratios of the samples , b/h and L/h, are assumed to be constant in the present study.

The application of the Buckingham's Π-Theorem to Eq. (9) yields the following relationship:

$$\frac{M}{h^{2.5}\sqrt{\mathcal{G}_C E_c}} = \Phi_1\left(\frac{\sigma_c h^{0.5}}{\sqrt{\mathcal{G}_C E_c}}, \rho_t \frac{\sigma_y h^{0.5}}{\sqrt{\mathcal{G}_C E_c}}, \vartheta \frac{E_c h^{0.5}}{\sqrt{\mathcal{G}_C E_c}}\right) \quad (9)$$

if h and $\sqrt{\mathcal{G}_C E_c}$ are assumed as the dimensionally independent variables. It is worth noting that the former parameter is representative of the size-scale of the specimen, whereas the latter is a material property. In particular, $\sqrt{\mathcal{G}_C E_c}$ can be physically interpreted as the concrete toughness in compression. Its expression, in fact, is analogously to that of the fracture toughness, K_{IC}, defined in terms of the fracture energy and the elastic modulus of the material. As a consequence, the dimensionless functional relationship for the proposed model becomes:

$$\tilde{M} = \Phi_1\left(N_C, N_P, \vartheta_n\right) \quad (10)$$

where:

$$N_P = \rho_t \frac{\sigma_y h^{0.5}}{\sqrt{\mathcal{G}_C E_c}} \quad (11)$$

and

$$N_C = \frac{\sigma_c h^{0.5}}{\sqrt{\mathcal{G}_C E_c}} \quad (12)$$

are the governing nondimensional numbers, $\tilde{M}$ is the nondimensional bending moment, and ϑ_n is the normalized rotation. According to Eq. (11), we expect that the structural response, in terms on nondimensional moment versus normalized rotation, is only a function of the dimensionless numbers N_P and N_C. In particular, physical similitude is predicted when the two dimensionless parameters are kept constant, although the single mechanical and geometrical properties vary.

5 INTERPRETATION OF NUMERICAL AND EXPERIMENTAL RESULTS ON THE BASIS OF DIMENSIONAL ANALYSIS

In this section, an original interpretation of numerical and experimental results is proposed in order to obtain a complete and exhaustive description of the effects of the materials and geometrical properties on the flexural behavior of reinforced concrete beams. On the basis of the analytical results obtained through Dimensional Analysis, in fact, the overall mechanical response is profitably analyzed through the two nondimensional numbers introduced before. The numerical simulations for values of N_P ranging from 0.049 up to 0.329, N_C being kept equal to 0.791, are shown in Figure 5. It is worth noting that, in practical applications, typical values for N_P range from 0.004 up to 0.360, whereas N_C varies from 0.2 up to 3.5. A clear decrement in the rotational capacity is evidenced with a reduction in the plastic plateau as the value of N_P increases. Such a trend can be easily interpreted through an increment in the steel percentage, ρ_t, which appears only in the expression of N_P and not in that of N_C. Note that the ultimate rotation is clearly identified by a softening or even a snap-back branch at the end of the plastic plateau, due to the nonlinear behavior of concrete in compression.

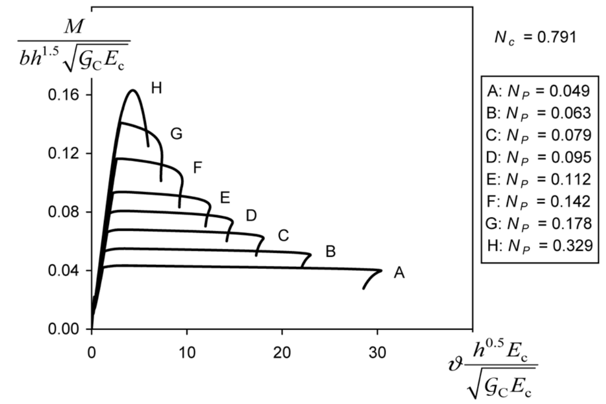

Figure 5. Nondimensional moment vs. normalized rotation diagrams for $N_C = 0.791$ and different values of N_P.

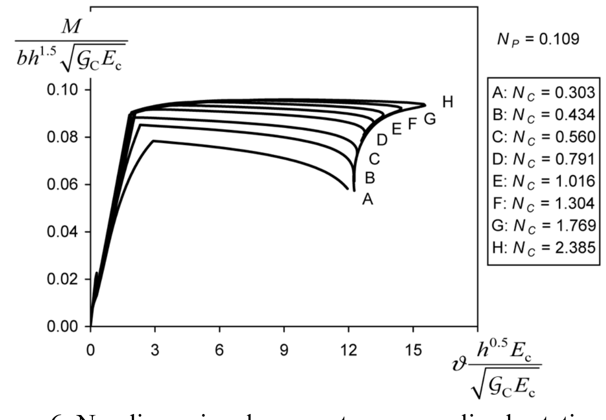

Figure 6. Nondimensional moment vs. normalized rotation diagrams for $N_P = 0.109$ and different values of N_C.

On the other hand, the curves in Figure 6 are related to values of N_C varying from 0.303 up to 2.385, with $N_P = 0.109$. In this case, the rotational capacity is an increasing function of N_C, as well as of the concrete compressive strength, σ_c. Correspondingly, a more unstable response after the ultimate rotation is also predicted by the occurrence of a sharper snap-back branch.

In order to give an experimental validation to the analytical and numerical approach proposed in the present paper, the bending tests carried out by Bosco and Debernardi (1993) on simply supported reinforced concrete beams with different sizes and loaded by three equal loads arranged symmetrically to the mid-span, are herein considered. The steel yielding strength is equal to 600 MPa, and the concrete compressive strength and elastic modulus are equal to 30.9 MPa and 30 GPa, respectively. The other geometrical and mechanical parameters are reported in Tab. 1. The plastic rotation, ϑ_{PL}, of the central beam portion characterized by a length to depth ratio equal to unity, as a function of the relative neutral axis position, x/d, is shown in Figure 7a. Such results evidence a different trend in the rotational capacity by varying the beam depth from 0.2 m up to 0.6 m. The shallower beams, in fact, exhibit a higher ductility than the deeper ones. On the contrary, such different trends collapse onto a narrow band in the normalized plastic rotation versus N_P diagram shown in Figure 7b. In this case, based on the curves shown in Figure 6, the nondimensional parameter N_C is not considered, since it exhibits a small variation for the considered beams (see Tab. 1). The results of the numerical simulations carried out with the proposed model are also represented in Figure 7b by the not filled-in symbols. A generally good agreement is obtained between numerical and experimental results. For low values of N_P, up to about 0.03, the global collapse is due to steel failure, and $\vartheta_{PL,n}$ is an increasing function of size and amount of steel reinforcement. On the contrary, for higher values of N_P, when the collapse is due to concrete crushing, $\vartheta_{PL,n}$ shows an opposite trend.

Table 1. Mechanical and geometrical parameters of the beams tested by Bosco & Debernardi (1993).

beam	b [mm]	h [mm]	ρ_t [%]	$\mathcal{G}_C$ [N/mm]	N_P	N_C	x/d	ϑ_{PL} [mrad]
T1A3			0.57		0.039	0.282	0.226	73.93
T2A3	100	200	1.13	50.0	0.078	0.282	0.335	64.64
T3A3			1.70		0.118	0.282	0.600	7.56
T4A3			0.28		0.033	0.564	0.115	67.06
T5A3	200	400	0.57	35.0	0.067	0.564	0.229	122.39
T6A3			1.13		0.013	0.564	0.462	14.82
T7A3			1.70		0.199	0.564	0.636	2.50
T8A3			0.13		0.016	0.496	0.108	23.47
T9A3	300	600	0.25	48.0	0.031	0.496	0.147	52.30
T10A3			0.57		0.069	0.496	0.237	32.41
T11A3			1.13		0.138	0.496	0.488	8.50

In order to highlight the different overall response evidenced by varying the beam size, a comparison in terms of moment–rotation diagram is shown in Figure 8 for three of the considered tests (see Carpinteri et al. 2009b for a more extensive comparison with the experimental results).

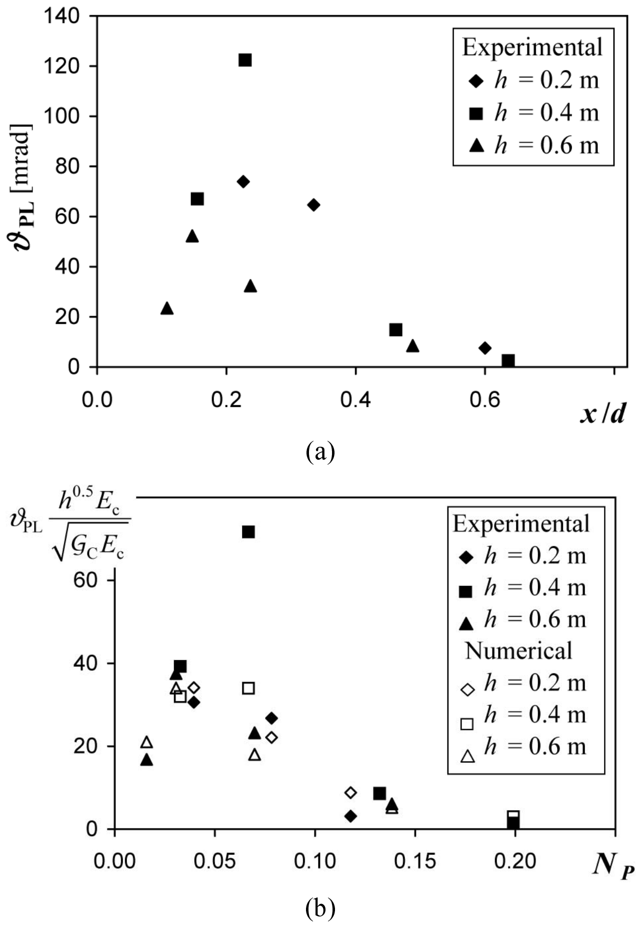

Figure 7. Experimental plastic rotations vs. x/d diagram (a); experimental and numerical normalized rotations vs. nondimensional number N_P diagram (b).

6 CONCLUSIONS

A numerical algorithm based on nonlinear fracture mechanics concepts both in tension and compression is introduced for the analysis of reinforced concrete beams in bending, with particular regard to the rotational capacity of plastic hinges. In this context, a new diagram for practical design purposes has been proposed to improve the current codes prescriptions and take into account the size-scale effects. Further improvements towards a simplification in the description of the overall response are obtained by the application of Dimensional Analysis to the proposed approach. The following main conclusions can be drawn from the analytical and numerical results:

1. The flexural behavior is not governed by the single values of the mechanical and geometrical parameters, but only by their combinations in two nondimensional numbers, N_P and N_C.
2. Physical similitude in the nondimensional moment versus normalized rotation diagram is predicted when the two dimensionless parameters are kept constant, although the single mechanical and geometrical properties vary.
3. As far as the rotational capacity is concerned, it can be evidenced that the normalized rotation is a decreasing function of N_P, N_C being kept constant, whereas it increases by increasing the value of N_C, N_P being kept constant. Such an evidence can be profitably used to give new and accurate descriptions of experimental results, as proved in Figure 7a, b. In particular, the diagram in Figure 7b permits to describe with a single curve the effect of structural dimension and steel reinforcement on the rotational capacity, whereas the analogous ones proposed by Model Code 90 and Eurocode 2 (2004), with different variables on the horizontal and vertical axis, completely disregard the size-scale effects.

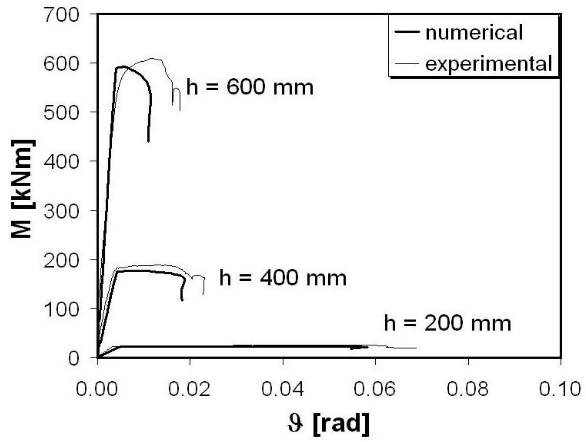

Figure 8. Comparison between numerical and experimental results for different beam depths and ρ_t = 1.13 %.

REFERENCES

Barenblatt, G.I. 1996. *Scaling, Self-Similarity, and Intermediate Asymptotics*. Cambridge (UK): Cambridge University Press.

Barenblatt, G.I. & Botvina, L.R. 1980. Incomplete self-similarity of fatigue in the linear range of fatigue crack growth. *Fatigue and Fracture of Engineering Materials and Structures* 3: 193-202.

Beeby, A.W. 1997. Ductility in reinforced concrete: why is it needed and how is it achieved?. *The Structural Engineer* 75: 311-318.

Bigaj, A.J. & Walraven, J.C. 1993. Size effect on rotational capacity of plastic hinges in reinforced concrete beams. *CEB Bulletin d'Information* 218: 7-23.

Bigaj, A.J. & Walraven, J.C. 2002. Size effect on plastic hinges of reinforced concrete members. *Heron* 47: 53-75.

Bosco, C. & Carpinteri, A. 1992. Fracture mechanics evaluation of minimum reinforcement in concrete structures. In A. Carpinteri (ed.), *Applications of Fracture Mechanics to Reinforced Concrete*: 347-377. Elsevier Applied Science.

Bosco, C. & Debernardi, P.G. 1993. Influence of some basic parameters on the plastic rotation of reinforced concrete elements. *CEB Bulletin d'Information* 218: 25-44.

Brincker, R., Henriksen, M.S., Christensen, F.A. & Heshe, G. 1999. Size effects on the bending behaviour of reinforced concrete beams. In A. Carpinteri (ed), *Minimum Reinforcement in Concrete Members*: 127-180. Oxford (UK): Elsevier Science Ltd.

Buckingham, E. 1915. Model experiments and the form of empirical equations. *ASME Transactions* 37: 263-296.

Burns, N.H. & Siess, Ch.P. 1966. Plastic hinging in reinforced concrete. *ASCE Journal of Structural Division* 92: 45-61.

Calvi, G.M., Cantù, E., Macchi, G. & Magenes, G. 1993. Rotation capacity of r.c. slabs as a function of steel properties. *CEB Bulletin d'Information* 218: 45-64.

Carpinteri, A. 1981a. Size effect in fracture toughness testing: A dimensional analysis approach. In: Analytical and Experimental Fracture Mechanics (Proc. of an International Conference, Roma, Italy, 1980): 785-797 Alphen an den Rijn: Sijthoff & Noordhoff.

Carpinteri, A. 1981b. Static and energetic fracture parameters for rocks and concretes. *Materials & Structures* 14: 151-162.

Carpinteri, A. 1981c. A fracture mechanics model for reinforced concrete collapse. In *Advanced Mechanics of Reinforced Concrete* (Proc. of a IABSE Colloquium, Delft, the Netherlands, 1981): 17-30. Delft: Delft University Press.

Carpinteri, A. 1982. Sensitivity and stability of progressive cracking in plain and reinforced cement composites. *International Journal of Cement Composites and Lightweight Concrete* 4: 47-56.

Carpinteri, A. 1984. Stability of fracturing process in RC beams. *Journal of Structural Engineering* 110: 544-58.

Carpinteri, A. 1991. Size-scale transition from ductile to brittle failure: structural response vs. crack growth resistance curve. *International Journal of Fracture* 51: 175-186.

Carpinteri, A. 1985. Interpretation of the Griffith instability as a bifurcation of the global equilibrium. In S.P. Shah (ed), *Application of Fracture Mechanics to Cementitious Composites*: 287-316. Dordrecht: Martinus Nijhoff Publishers.

Carpinteri, A. 1989. Size effects on strength, toughness, and ductility. *Journal of Engineering Mechanics* 115: 1375-1392.

Carpinteri, A., Ferro, G. & Ventura, G. 2003. Size effects on flexural response of reinforced concrete elements with a nonlinear matrix. *Engineering Fracture Mechanics* 70: 995-1013.

Carpinteri, A., Corrado, M., Paggi, M. & Mancini, G. 2007. Cohesive versus overlapping crack model for a size effect analysis of RC elements in bending. In A. Carpinteri, P. Gambarova, G. Ferro, & G. Plizzari (eds), *Fracture Mechanics of Concrete Structures*: 655-663. London: Taylor & Francis.

Carpinteri, A., Corrado, M., Paggi, M. & Mancini, G. 2009a. New model for the analysis of size-scale effects on the ductility of reinforced concrete elements in bending. *Journal of Engineering Mechanics* 135: 221-229.

Carpinteri, A., Corrado, M., Paggi, M. & Mancini, G. 2009b. A numerical approach to modelling size effects on the flexural ductility of RC beams. *Materials & Structures*. doi: 10.1617/s11527-008-9454-y

CEN TC/250 2004. *Eurocode 2: Design of Concrete Structures, Part 1-1: General Rules and Rules for Buildings*. Brussels.

Ciavarella, M., Paggi, M. & Carpinteri, A. 2008. One, no one, and one hundred thousand crack propagation laws: A generalized Barenblatt and Botvina dimensional analysis approach to fatigue crack growth. *Journal of the Mechanics and Physics of Solids* 56: 3416-3432.

Comité Euro-International du Béton. 1993. CEB-FIP Model Code 1990. In *CEB Bulletin d'Information* 213/214. Lausanne: Thomas Telford Ltd.

Corley, G.W. 1966. Rotational capacity of reinforced concrete beams. *Journal of Structural Division* 92: 121-146.

Cosenza, E., Greco, C. & Manfredi, G. 1991. Theoretical evaluation of inelastic rotations and displacements in the reinforced concrete monodimensional elements. (in Italian) *Atti dell'Accademia Nazionale dei Lincei* Serie IX, Vol. II, Fascicolo 3: 249-258.

Eligehausen, R. & Langer, P. 1987. Rotation capacity of plastic hinges and allowable moment redistribution. *CEB Bulletin d'Information* 175: I 7.9-I 7.27.

Hillerborg, A. 1990. Fracture mechanics concepts applied to moment capacity and rotational capacity of reinforced concrete beams. Engineering Fracture Mechanics 35:233-240.

Hillerborg, A., Modeer, M. & Petersson, P.E. 1976. Analysis of crack formation and crack growth in concrete by means of fracture mechanics and finite elements. *Cement and Concrete Research* 6: 773-782.

Jansen, D.C. & Shah, S.P. 1997. Effect of length on compressive strain softening of concrete. Journal of Engineering Mechanics 123: 25-35.

Langer, P. 1998. *Verdrehfähigkeit plastizierter Tragwerksbereiche im Stahlbetonbau*. (in German) PhD Thesis, University of Stuttgart, Institut für Werkstoffe im Bauwesen, Berlin.

Markeset, G. 1993. *Failure of concrete under compressive strain gradients*. PhD Thesis. Trondheim: The Norwegian Institute of Technology.

Mattock, A.H. 1965. Rotational capacity of hinging regions in reinforced concrete beams. In *Abstracts of the Flexural Mechanics of Reinforced Concrete*: 143-181. ASCE-ACI International Symposium, ACI SP-12.

Phatak, D.R. & Deshpande, N.P. 2005. Prediction of 28 days compressive strength of 53-grade cements using dimensional analysis. *Journal of Materials in Civil Engineering* 17: 733-735.

Phatak, D.R. & Dhonde, H.B. 2003. Dimensional analysis of reinforced concrete beams subjected to pure torsion. *Journal of Structural Engineering* 129: 1559-1563.

Pecce, M. & Fabbrocino, G. 1999. Plastic rotation capacity of beams in normal and high-performance concrete. *ACI Structural Journal* 96: 290-296.

Pommerening, D. 1996. *Ein beitrag zum nichtlinearen Materialverhalten und zur Schnittgrößenermittlung im Massivbau*. (in German) PhD Thesis, Technischen Hochschule Darmstad,

Ruiz, G., Elices, M. & Planas, J. 1999. Size effects and bond-slip dependence of lightly reinforced concrete beams. In A. Carpinteri (ed), *Minimum Reinforcement in Concrete Members*: 127-180. Oxford (UK): Elsevier Science Ltd.

Siviero, E. 1974. Rotation capacity of monodimensional members in structural concrete. *CEB Bulletin d'Information* 105: 206-222.

Shin, S., Ghosh, S.K. & Moreno, J. 1989. Flexural ductility of ultra-high-strength concrete members. *ACI Structural Journal* 86: 394-400.

Somes, N.F. 1966. Technical report: moment-rotation characteristics of prestressed concrete members, StageI: rectangular sections. *TRA/398*. London: Cement and Concrete Association.

Suzuki, M., Akiyama, M., Matsuzaki, H. & Dang, T.H. 2006. Concentric loading test of RC columns with normal- and high-strength materials and averaged stress-strain model for confined concrete considering compressive fracture energy. In *Proceedings of the 2nd fib Congress*, Naples, Italy, June 5-8, 2006, (CD-ROM).

van Mier, J.G.M. 1984. *Strain-softening of Concrete under Multiaxial Loading Conditions*. PhD Thesis, Eindhoven: University of Technology.